International Journal of Nanomedicine

Dovepress
open access to scientific and medical research

Open Access Full Text Article

ORIGINAL RESEARCH

RETRACTED ARTICLE: Antimicrobial activity of silver nanoparticles encapsulated in poly-*N*-isopropylacrylamide-based polymeric nanoparticles

This article was published in the following Dove Press journal:
International Journal of Nanomedicine

Muhammad Qasim[1]
Nopphadol Udomluck[1]
Jihyun Chang[1]
Hansoo Park[1]
Kyobum Kim[2]

[1]School of Integrative Engineering, Chung-Ang University, Seoul, [2]Division of Bioengineering, Incheon National University, Incheon, Republic of Korea

Abstract: In this study, we analyzed the antimicrobial activities of poly-*N*-isopropylacrylamide (pNIPAM)-based polymeric nanoparticles encapsulating silver nanoparticles (AgNPs). Three sizes of AgNP-encapsulating pNIPAM- and pNIPAM-AA_2-based polymeric nanoparticles were fabricated. Highly stable and uniformly distributed AgNPs were encapsulated within polymeric nanoparticles via in situ reduction of $AgNO_3$ using $NaBH_4$ as the reducing agent. The formation and distribution of AgNPs was confirmed by UV-visible spectroscopy, transmission electron microscopy, and inductively coupled plasma optical emission spectrometry, respectively. Both polymeric nanoparticles showed significant bacteriostatic activities against Gram-negative (*Escherichia coli*) and Gram-positive (*Staphylococcus aureus*) bacteria depending on the nanoparticle size and amount of $AgNO_3$ used during fabrication.

Keywords: pNIPAM, silver nanoparticles, antimicrobial activities, surface charge

Introduction

Various bacteria and fungi cause postsurgical infections. Such infections are frequently associated with medical implants, including prosthetic joints and fracture fixation materials.[1–3] Because of the slow progress of such infections, detecting them at an early stage is challenging. In the absence of an effective antibiotic, failure to treat postsurgical infections with classical antibiotics is a serious global issue.[1,4,5] A bacterial strain carrying the *NDM-1* gene was recently reported to be resistant to strong antibiotics; thus, microbial drug resistance and the lack of effective antimicrobial agents pose great challenges.[6]

Non-conventional treatments for microbial infections include antimicrobial peptides, small molecule inhibitors, naturopathic therapy, phytotherapy, and metallic particles.[7–9] Previously, the use of silver nanoparticles (AgNPs) was suggested for eliminating microbial infections.[10] Broad-spectrum antimicrobial activities of Ag against pathogens, including both Gram-positive and Gram-negative bacteria, have been reported.[11,12] Ag was complexed with other materials to give them with antibacterial properties. For example, the antimicrobial activity of Ag-impregnated nylon fibers against *Staphylococcus aureus* and *Candida albicans* was evaluated for wound dressing.[13,14] AgNPs have also been used to treat *Escherichia coli* because of their ability to damage bacterial cell walls.[15] Currently, AgNPs in burn ointments, wound dressings, and Ag-coated medical devices such as catheters, vascular grafts, and endotracheal tubes are used to prevent and treat bacterial infections.[16–18]

Correspondence: Hansoo Park
School of Integrative Engineering, Chung-Ang University, 221 Heuk Seok-Dong, Dongjak-Gu, Seoul, Republic of Korea
Tel +82 2 820 5940
Fax +82 2 813 8159
Email heyshoo@cau.ac.kr

Kyobum Kim
Division of Bioengineering, Incheon National University, 119 Academy-ro, Yeonsu-gu, Incheon, Republic of Korea
Tel +82 32 835 8297
Fax +82 32 835 0736
Email kyobum.kim@inu.ac.kr

Polymeric nanoparticles are an excellent vehicle for AgNP delivery because they can easily be modified according to the target site; moreover, their size, morphology, and surface charge can be controlled by changing the ratio of monomer to cross-linker during nanoparticle fabrication.[19,20] Another advantage of encapsulating AgNPs inside a polymeric nanoparticle is that nanoparticles distributed in a polymeric nanoparticle show low aggregation.[21,22] Moreover, polymeric nanoparticles reduce concerns regarding the cytotoxicity of AgNPs because the gel limits the direct exposure of a patient's cells to AgNPs and release AgNPs slowly.[23,24] Previously, it was reported that encapsulation of AgNPs inside a polymeric nanoparticle did not affect the size and morphology of the nanocomposite.[25] Polymeric nanoparticles are an attractive vehicle for sustained AgNP release during local therapy because of their tunable size, numerous functional groups, thermo-responsiveness, high loading capacity, good stability, biocompatibility, and anionic charge.[21,24,26]

In this study, we fabricated three sizes of two polymeric nanoparticle types: poly-*N*-isopropylacrylamide (pNIPAM) and pNIPAM-NH_2. In each polymeric nanoparticle, we encapsulated three different concentrations of AgNPs using a water-soluble reducing agent. We then examined the effects of polymeric nanoparticle surface charge and AgNP concentration on antimicrobial activity against Gram-negative (*E. coli*) and Gram-positive (*S. aureus*) bacteria. Our aim was to increase antimicrobial activity by encapsulating AgNPs inside a polymeric nanoparticle to limit the cell uptake and cytotoxicity. Our AgNP-encapsulated polymeric nanoparticles (AgNP-pNIPAM/pNIPAM-NH_2 nanoparticles) showed significant bacteriostatic activities against *E. coli* and *S. aureus* that were dependent on nanoparticle size and $AgNO_3$ concentration. The resulting AgNP-pNIPAM/pNIPAM-NH_2 polymeric nanocomposite can be developed for antimicrobial biomedical engineering applications.

Materials and methods

Materials

NIPAM, $AgNO_3$, NaOH, sodium dodecyl sulfate, and $NaBH_4$ were purchased from Sigma-Aldrich Co. (St Louis, MO, USA) and used after further purification through recrystallization. Ammonium persulfate (APS), *N,N*-methylenebisacrylamide (BIS), and *N*-(3-aminopropyl) methacrylamide hydrochloride (APMAAHC) were purchased from Polysciences (Warrington, PA, USA). Luria-Bertani (LB) broth medium was purchased from Oxoid (Basingstoke, UK). *E. coli* (25922) and *S. aureus* (25923) were purchased from ATCC (Manassas, VA, USA). DMEM containing glucose, phosphate-buffered saline, fetal bovine serum, penicillin G (pen; 10,000 U/mL), streptomycin (strep; 100 µg/mL), and amphotericin B (AmB; 25 µg/mL) were purchased from GE Healthcare Life Sciences (Little Chalfont, UK). Human adipose tissue was obtained from the Korea Cancer Center Hospital under the guidelines of the Institutional Review Board at Chung-Ang University (Seoul, South Korea). MTT and DMSO were purchased from Sigma-Aldrich Co. Deionized water (DW) was used to prepare solutions and for washing. All chemicals were used as received without further purification.

Synthesis of pNIPAM/pNIPAM-NH_2 nanoparticles

pNIPAM nanoparticles were fabricated by conventional radical polymerization of NIPAM.[28,29] Depending on the NIPAM to cross-linker ratio, three different sizes of pNIPAM nanoparticles (between 200–500 nm) were prepared. Specifically, 0.95 g of NIPAM with different amounts of BIS (0.026 g for 50:1, 0.013 g for 100:1, and 0.0065 g for 200:1) was dissolved in 195 mL DW, and the resulting solutions were transferred into a three-necked round-bottomed flask with a constant supply of argon gas. Sodium dodecyl sulfate was added in the same ratio as BIS as a surfactant. The solution was heated to 58°C–65°C with a constant supply of argon gas for 1 h. Next, 5 mL of APS solution (0.12 g of APS dissolved in 5 mL of DW) was injected into the solution to initiate polymerization and the reaction was allowed to proceed for 4 h.[30] Argon gas was purged through the solution until the end of the reaction to avoid any contact with oxygen, which may intercept radicals and disrupt polymerization. The resulting dispersion was dialyzed in DW using a porous membrane (6,000–8,000 Da molecular weight cutoff) and freeze-dried. The resulting pNIPAM-based nanoparticles are referred to as G1, G2, and G3, representing the nanoparticles prepared using three NIPAM:BIS ratios (0.0065 g BIS for 200:1, 0.013 g BIS for 100:1, and 0.026 g BIS for 50:1, respectively), as shown in Figure 1A. To fabricate polymeric nanoparticles with an amine (NH_2) group, 0.065 g of APMAAHC was added to the three different NIPAM:BIS ratio reaction solutions, creating three different sizes of pNIPAM-NH_2 nanoparticles. The resulting pNIPAM-NH_2-based polymeric nanoparticles were similarly referred to as G1, G2, and G3, as shown in Figure 1B. The sizes of the prepared polymeric nanoparticles were characterized by dynamic light scattering (DLS).

Preparation of AgNP-polymeric nanoparticles

To encapsulate AgNPs inside the polymeric nanoparticles, 30 mg of each polymeric nanoparticle (ie, G1, G2, and G3

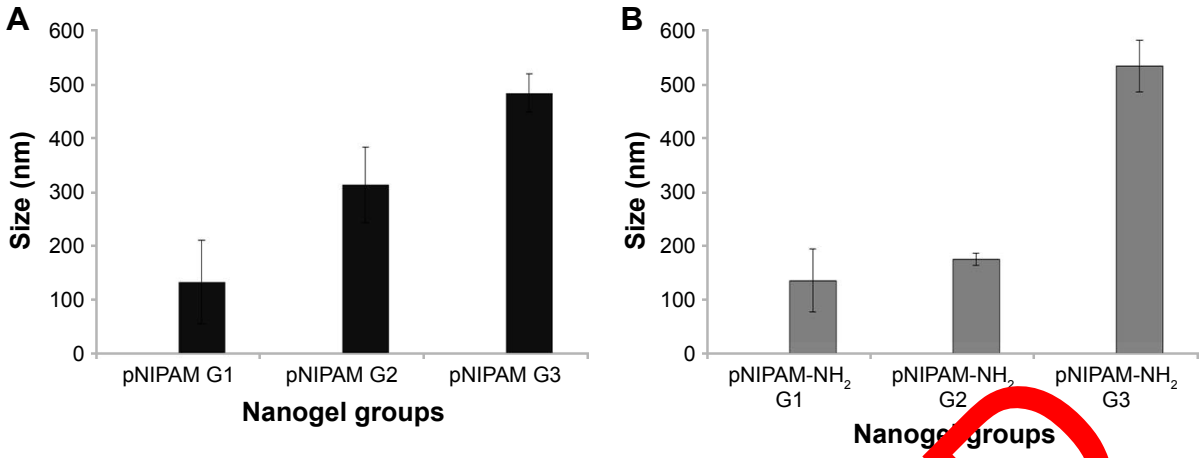

Figure 1 Average sizes of poly-*N*-isopropylacrylamide (pNIPAM) nanoparticle groups G1–G3 (**A**), and average sizes of pNIPAM-NH$_2$ nanoparticle groups G1–G3 (**B**).

with and without NH_2) was first incubated in 10 mM $NaBH_4$ solution in DW (5 mL) for 5 h. Next, the solutions were mixed with freshly prepared $AgNO_3$ solution (pH 7.0, 5 mL) and further incubated for 5 h at room temperature.[31] Before use, the pH of the $AgNO_3$ solutions was adjusted to pH 7 with NaOH and a pH meter. The $AgNO_3$ and polymeric nanoparticle solutions were centrifuged at 11,000 rpm for 40 min and then washed with DW. This process was repeated three times to remove unreduced Ag^+ or excess AgNPs located outside the polymeric nanoparticle network. Finally, 5 mL of DW was added to each sample before storing it at 8°C. After washing, the AgNP pNIPAM/pNIPAM-NH_2 nanoparticle composites were characterized by UV-visible spectroscopy, transmission electron microscopy (TEM), and inductively-coupled plasma optical emission spectrometry (ICP-OES). The overall fabrication scheme was described in Figure 2.

Characterization of AgNP-encapsulating polymeric nanoparticles

The sizes of three fabricated pNIPAM and pNIPAM-NH_2 polymeric nanoparticles were determined by DLS using a Zetasizer Nano ZS (Malvern Instruments, Malvern, UK). The mean particle diameter (z-average) and particle size distribution (polydispersity index) were measured at 25°C. The spectral absorption of the three AgNP-encapsulating pNIPAM and pNIPAM-NH_2 nanoparticle size groups was assessed using a UV-visible spectrophotometer (Synergy™ HT reader, BioTek Instruments, Winooski, VT, USA) in the range of 300–600 nm.[27] All experiments were performed in triplicate to determine mean and SD values. The compositions of the resulting AgNP-encapsulating pNIPAM and pNIPAM-NH_2 nanoparticle size groups were determined by ICP-OES. The morphological characteristics of the AgNP-encapsulating pNIPAM and pNIPAM-NH_2 nanoparticle groups were observed by high-resolution TEM (JEM 3010, JEOL, Tokyo, Japan). For TEM, a drop of AgNP-encapsulating polymeric nanoparticles solution in DW was placed on a copper grid and allowed to dry at room temperature, and then placed in the sample holder of the TEM instrument and analyzed.

Assessment of antimicrobial activity

Liquid culture

The antimicrobial activities of the prepared AgNP-polymeric nanoparticles against *E. coli* and *S. aureus* were investigated. All bacterial cultures were performed in LB broth. To promote the transition of bacterial cultures into the exponential growth phase, single colonies of *E. coli* or *S. aureus* were transferred to separate flasks containing LB broth and incubated overnight at 37°C with shaking at 175 rpm, and then diluted to 10^8 CFU/mL based on the OD at 600 nm (OD_{600}=1). To evaluate the antimicrobial activities of the AgNP

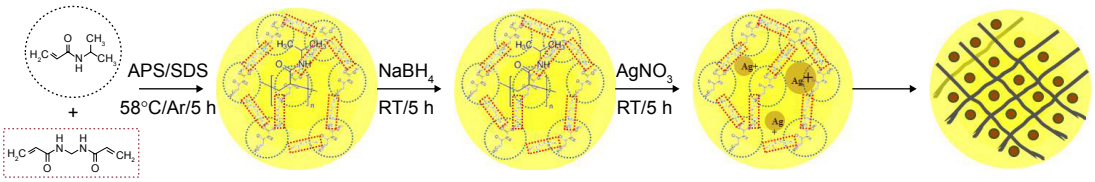

Figure 2 Schematic diagram of the synthesis of silver nanoparticle (AgNP)-encapsulated poly-*N*-isopropylacrylamide (pNIPAM)-based nanoparticle platforms.
Abbreviations: APS, ammonium persulfate; RT, room temperature; SDS, sodium dodecyl sulfate.

pNIPAM/pNIPAM-NH_2 nanoparticle size groups, 40 µL of each polymeric nanoparticle-AgNP composite (G1, G2, and G3 with and without NH_2) were added to 160 µL of bacterial suspension (10^8 CFU/mL) during the exponential growth phase in 96-well plates, and the samples were incubated at 37°C. Pure cultures were used as positive controls and culture media without cells were used as a negative control. All groups were cultured in triplicate. Bacterial growth was monitored by determining the OD of the bacterial suspension at 600 nm[4] and the OD_{600} values were recorded at 0, 1, 2, 3, 4, 5, and 24 h of incubation.

Plate diffusion method

To investigate the antimicrobial activity of AgNPs encapsulated in nanogels on solid media, *E. coli* and *S. aureus* (1×10^6 cells/mL) were cultured on MH agar plates and the plates were dried at room temperature. A well, 8 mm in diameter, was made in each plate by gel puncture. Next, 1 mg/mL of each nanogel with AgNPs was dissolved in autoclaved distilled water and 0.5 mL of this solution was applied to the plates. Each test was performed in triplicate and a pure bacterial culture was used as a control. The plates were incubated at 37°C for 24 h. Antimicrobial activity was measured as the average diameter (mm) of the zone of inhibition around each well.[32]

X-ray photoelectron spectroscopy (XPS) analysis

XPS was performed using a Leybold [illegible] Max[illegible] surface analysis system (Leybold, Cologne, Germany) operated with an Mg Kα source, 200 W. Prior to XPS analysis, all samples were thoroughly dried under vacuum. Data analysis was carried out using the Origin analysis programs. The binding energy scales of the high resolution spectra were calibrated by assigning the most intense C1s high resolution peak a binding energy of 285.08 eV (C–C) and 287.58 eV (C=O). A linear function was used to model the background.

Cytotoxicity assay

The cytotoxicities of the AgNP-polymeric nanoparticles to human adipose stem cells (hASCs) were determined by the MTT assay. The study was approved by the ethical review board of Chung Ang University and prior informed consent was signed by the tissue donor. The hASCs were cultured in DMEM containing 10% fetal bovine serum and 1% antibiotic-antimycotic solution (pen/strep/AmB) at room temperature under a 5% CO_2 atmosphere in a humidified incubator. A cell suspension (80 µL; 5,000 cells/well) was mixed with 20 µL of AgNP-polymeric nanoparticles on a 96-well plate for the MTT assay. A suspension of hASCs (80 µL) with 20 µL of DW and no nanoparticle was seeded as a positive control. In a different plate, hASC suspensions containing 20 µL of each size group of the pNIPAM and pNIPAM-NH_2 AgNP-nanoparticles were seeded. Each size group (G1, G2, and G3 with and without NH_2) was tested in triplicate.

According to the instructions from the MTT assay supplier (Sigma-Aldrich Co.), after incubating the cultures for 48 h, 10 µL of AmB solution was added to each well and incubated for 4 h. Next, 0.1 mL of isopropanol with 0.04 N hydrochloric acid was added to each well. All solutions in the wells were thoroughly mixed using repeated pipetting with a multichannel pipette. Absorbance was recorded using a Synergy™ HT microplate reader (BioTek Instruments) at 570 and 690 nm for quantification.

Statistical analysis

Absorbance data of the cytotoxicity of the AgNP-polymeric nanoparticles were expressed as the mean ± SD (n=3) in Figure 3. One-way analysis of variance (ANOVA) with Tukey's multiple comparison test was performed to determine statistical significance, by using Graphpad Prism software (La Jolla, CA, USA). A value of $p<0.05$ was considered to denote statistical significance as compared with the positive control group.

Results

Characterization of AgNP encapsulating pNIPAM and pNIPAM-NH_2 polymeric nanoparticles

The sizes of the prepared pNIPAM/pNIPAM-NH_2 polymeric nanoparticles were determined by DLS. The average sizes of the G1, G2, and G3 pNIPAM nanoparticles were 131±78, 312±71, and 483±35 nm, respectively (Figure 1A), while the average sizes of the G1, G2, and G3 pNIPAM-NH_2 nanoparticles were 135±59, 174±10, and 532±48 nm, respectively (Figure 1B).

UV-visible absorption spectrum exhibited a proper encapsulation of AgNP in polymeric nanoparticles (Figures 4 and 5). Previous studies showed that UV-visible absorption spectrum results are sensitive to the formation of AgNPs and that the absorption peaks depend on particle diameter and shape.[25,34] The AgNP absorption band is in the 400–500 nm range.[35] Previous results have suggested that AgNPs of smaller diameters are obtained at larger absorption doses.[36] Figures 4A and 5A show the UV-visible spectra of AgNPs encapsulated in the pNIPAM and pNIPAM-NH_2

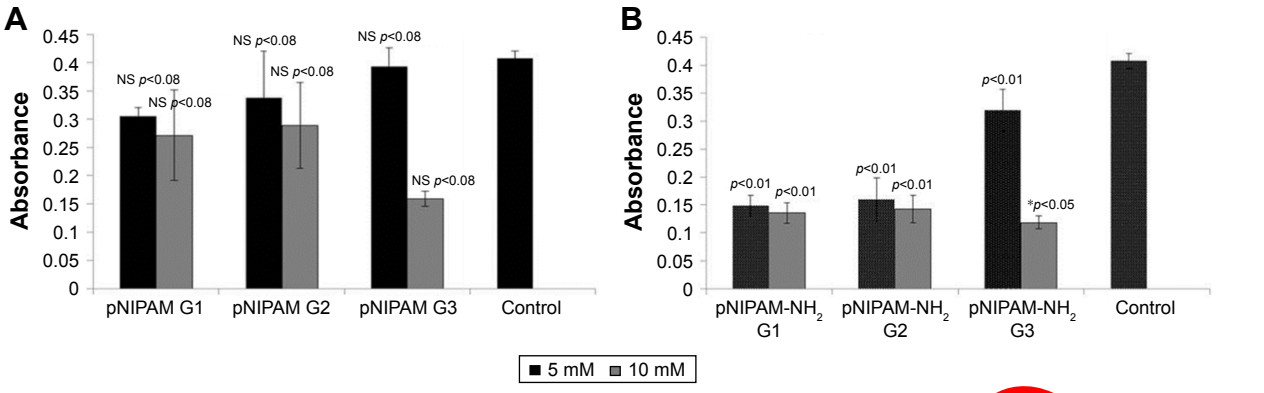

Figure 3 (**A**) Cytotoxicity of silver nanoparticle (AgNP)-encapsulated poly-*N*-isopropylacrylamide (pNIPAM) nanoparticle groups and (**B**) AgNP encapsulated pNIPAM-NH_2 nanoparticle groups against human adipose stem cells after 48 h.
Note: *p-value ($p<0.05$) indicates a significant difference as compared with the control (ie, absorbance from the cell treated with nanoparticles).
Abbreviation: NS, non significant.

AgNP-nanoparticles. The results confirmed that the AgNP fabrication process was consistent in terms of the spectral absorbance of the gels. The UV-visible spectra of our AgNP-polymeric nanoparticles showed a maximum absorbance at 437 nm, as shown in Figures 4A and 5A, which confirms the encapsulation of AgNP inside the polymeric nanoparticles. In previous studies, AgNPs (2–5 nm) embedded in polymer hydrogels exhibited the same absorption bands in poly(methyl methacrylate-co-butyl acrylate-co-acrylic acid), polyethylenimine, and silica gels.[34,37,38] In the present

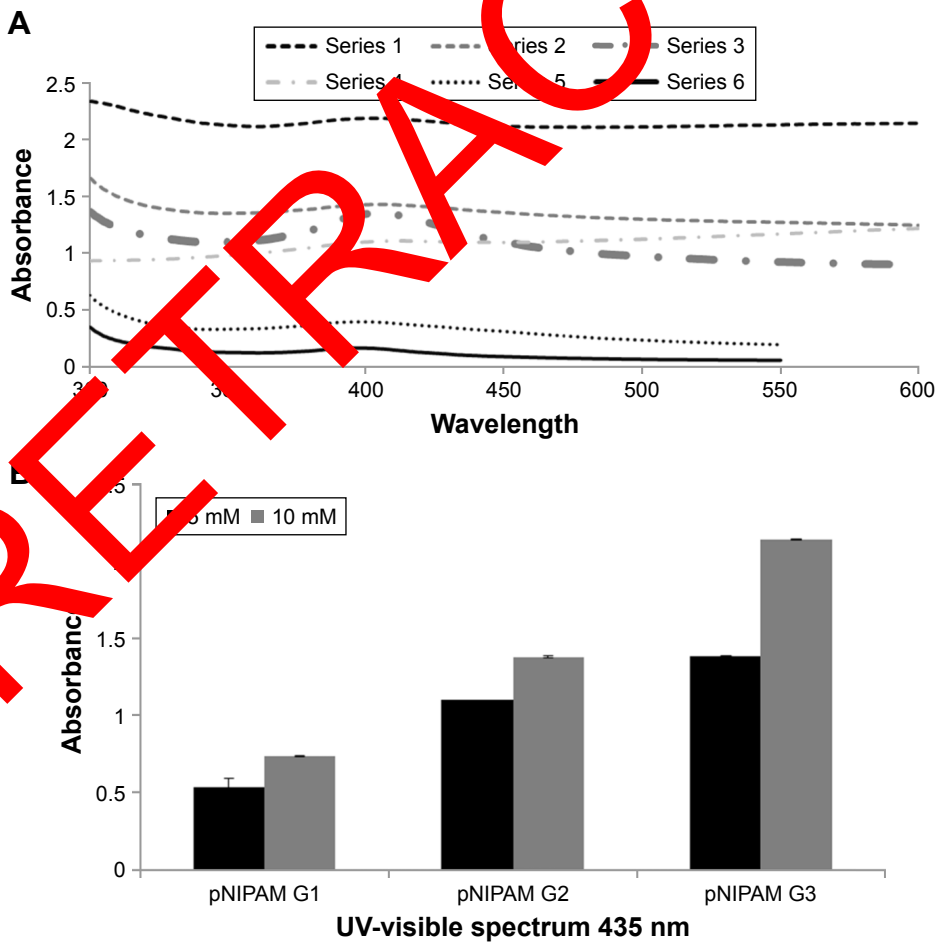

Figure 4 (**A**) UV-visible spectra of silver nanoparticle (AgNP)-encapsulated poly-*N*-isopropylacrylamide (pNIPAM) nanoparticle groups G1–G3, and (**B**) Ag peak absorbance at 435 nm in gels containing 5 and 10 mM concentrations of $AgNO_3$.

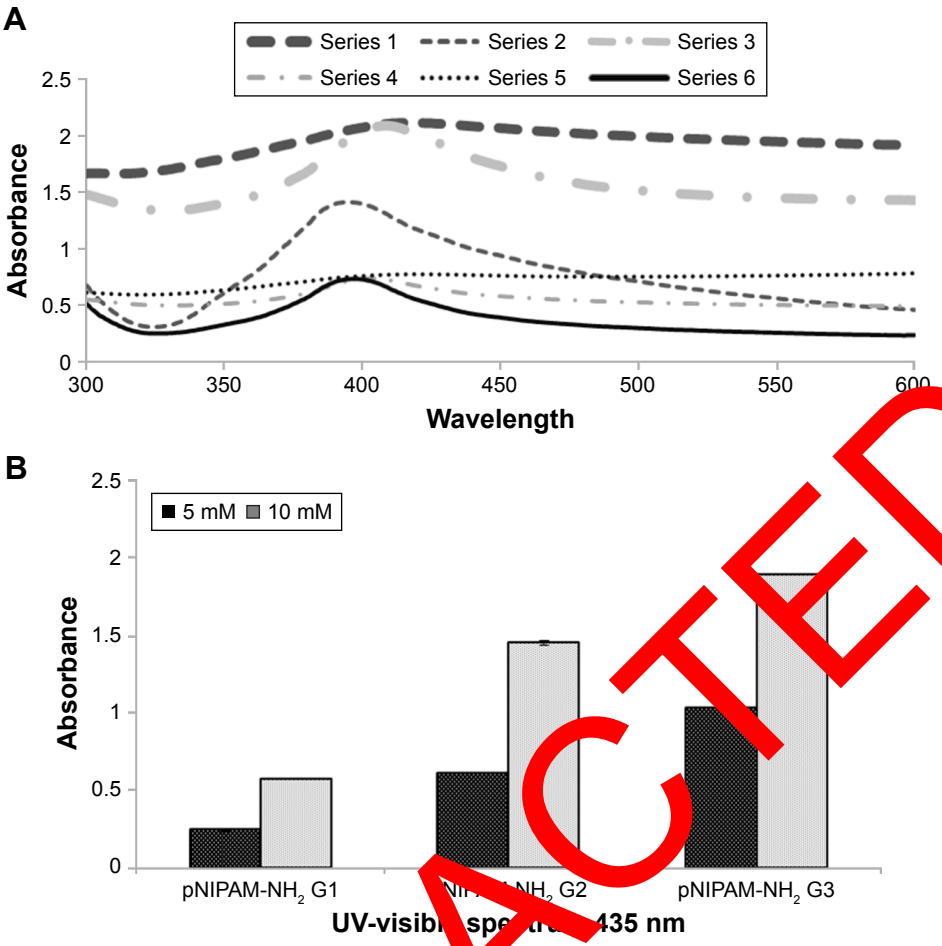

Figure 5 (**A**) UV-visible spectra of silver nanoparticle (AgNP)-encapsulated poly-N-isopropylacrylamide (pNIPAM)-NH_2 nanoparticle groups G1–G3, and (**B**) Ag peak absorbance at 435 nm in gels containing 5 and 10 mM concentrations of $AgNO_3$.

study, all absorption peaks were similar and all AgNP-polymeric nanoparticles showed maximum absorption at 437 nm (Figures 4A and 5A), suggesting that the AgNPs encapsulated within the AgNP-polymeric nanoparticles are similar in size and morphology. Furthermore, the absence of a peak at 560 nm confirms that there was no AgNP aggregation or cluster formation inside the AgNP-polymeric nanoparticles.[39]

Using the current method, we obtained a homogeneous distribution of AgNPs throughout each polymeric nanoparticle. Moreover, the Ag salts loaded in the cross-linked AgNP-polymeric nanoparticles were extensively reduced by $NaBH_4$, after which the color of the solution quickly changed to opaque brown.[40] These results indicate that the AgNPs were completely encapsulated within the AgNP-polymeric nanoparticles with strong localization and stabilization provided by the three-dimensional network within the polymeric nanoparticles. In contrast, polymer functional groups such as –OH, –CONH, and –COOH promote the stabilization of AgNPs through surface adsorption.[20] Figures 4B and 5B show the changes in absorbance for different concentrations of $AgNO_3$ (5 and 10 mM) in the pNIPAM and pNIPAM-NH_2 AgNP-nanoparticles. The color of the AgNP polymeric nanoparticle solution was dependent on the concentration of $AgNO_3$. With the higher $AgNO_3$ concentration (10 mM), the color of the solution changed from light brown to dark brown, and the UV-visible spectrum peak at 437 nm was larger. The absorption peaks at 435 nm, as shown in Figures 4A and 5A, represent the characteristic peaks of surface plasmon resonance absorption by AgNPs.

Surface morphology of the resulting nanoparticles was evaluated using TEM (Figures 6 and 7). The images indicated that the morphologies for pNIPAM and pNIPAM-NH_2 AgNP-nanoparticles prepared with 5 or 10 mM $AgNO_3$ clearly depicted the spherical surfaces of the nanoparticles. AgNPs ranging from 1 to 35 nm in diameter were visible inside the polymeric nanoparticles (Figure S1A and B). The size of the AgNPs changed with the concentration of $AgNO_3$ used during fabrication, which affects the nanoparticle's internal network and surface charge.[4] The pNIPAM-NH_2

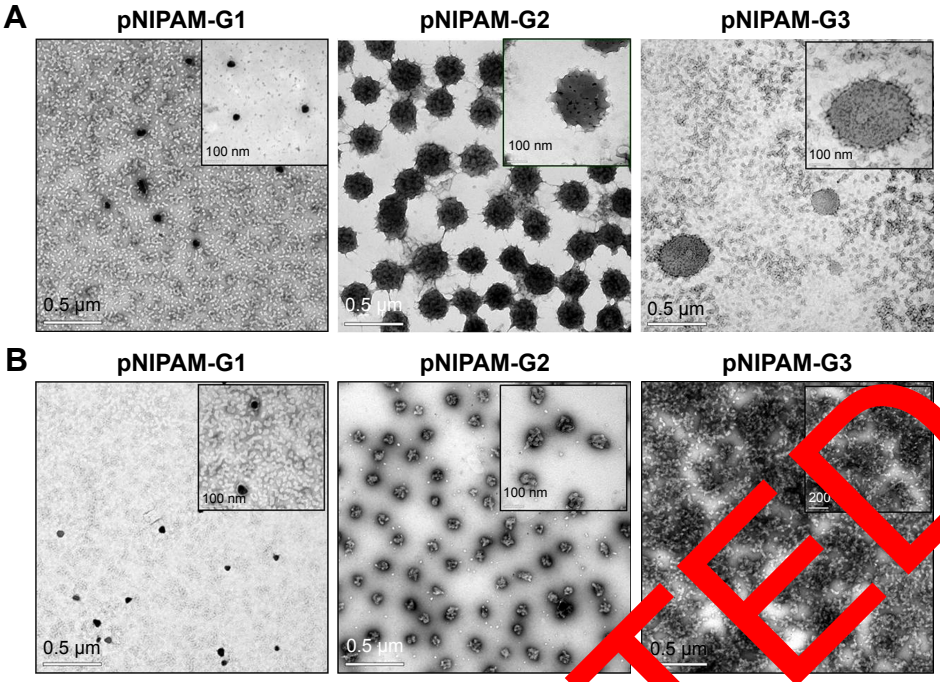

Figure 6 Representative transmission electron microscopy micrographs of silver nanoparticle (AgNP)-encapsulated poly-*N*-isopropylacrylamide (pNIPAM) nanoparticles fabricated with two different concentrations of silver salt, (**A**) 5 mM $AgNO_3$ and (**B**) 10 mM $AgNO_3$.
Note: The difference in retention of silver in nanocomposite after washing was confirmed by inductively-coupled plasma optical emission spectrometry analysis.

AgNP-nanoparticles contained larger AgNPs than the pNIPAM AgNP-nanoparticles due to the extra positive charge over the pNIPAM-NH_2 surface as shown in Figures 6 and 7.

Surface chemistry

To confirm functionalization of amine group on pNIPAM polymer, XPS analysis was performed. The XPS spectra of pNIPAM-functionalized samples are shown in Figure 8.

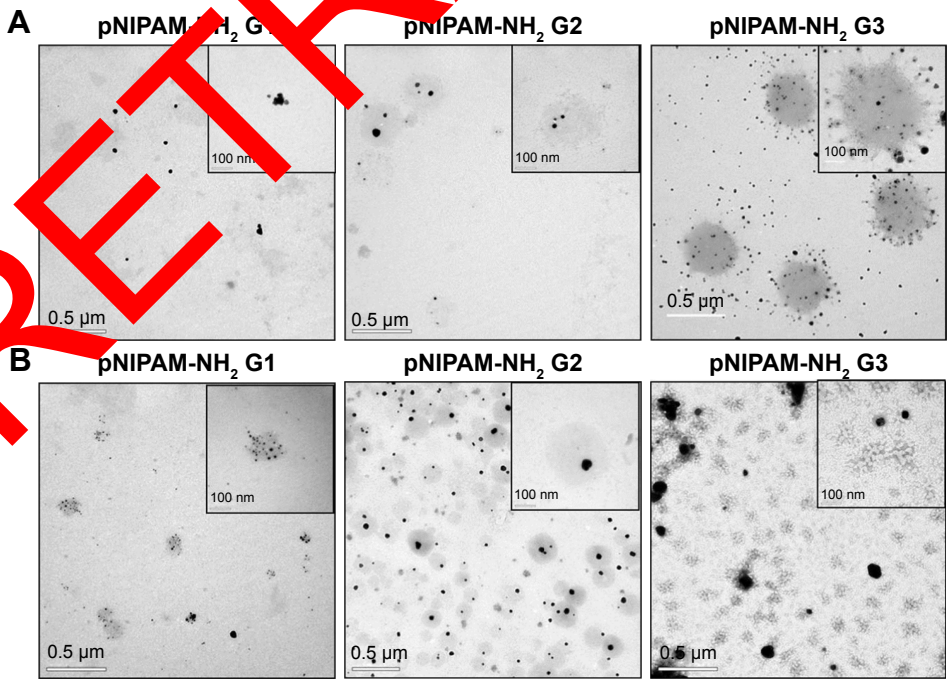

Figure 7 Representative transmission electron microscopy micrographs of silver nanoparticle (AgNP)-encapsulated poly-*N*-isopropylacrylamide (pNIPAM)-NH_2 nanoparticles fabricated with two different concentrations of silver salt, (**A**) 5 mM $AgNO_3$ and (**B**) 10 mM $AgNO_3$.
Note: The difference in retention of silver in nanocomposite after washing was confirmed by inductively-coupled plasma optical emission spectrometry analysis.

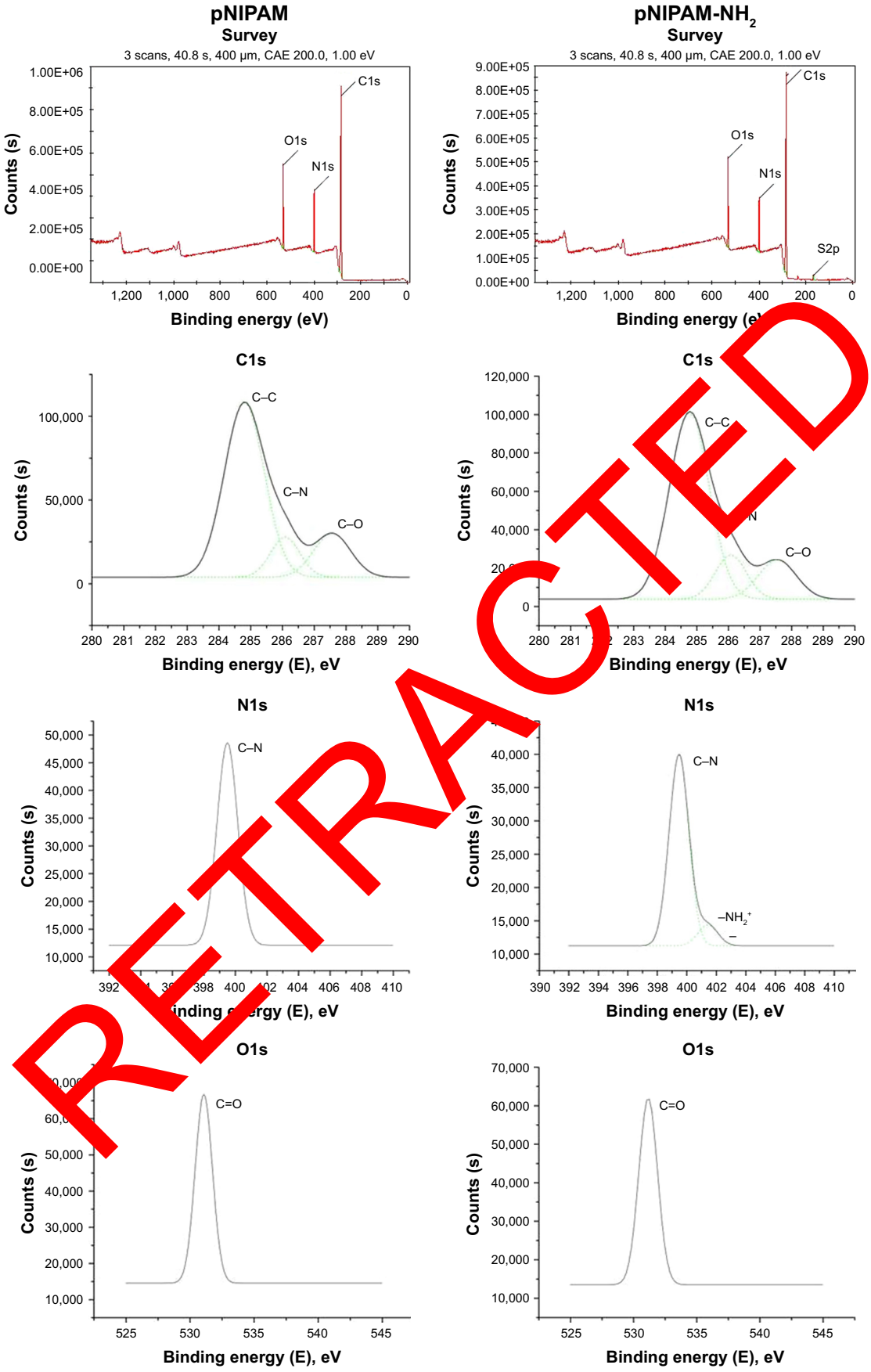

Figure 8 X-ray photoelectron spectroscopy spectra of poly-*N*-isopropylacrylamide (pNIPAM) (top) and pNIPAM-NH_2 (bottom), condition G1.
Notes: The curved-fitted spectra (black) are superimposed on the experimental data. The peaks of each coordination species are labeled and shown within the curve-fitted spectra.

The high resolution C1s, O1s, N1s spectra (to determine molecular bonding environment), were obtained, and done with curve fitting function in Origin software. For the C1s core-level, the typical characteristics of the amide groups comprising the backbone of the pNIPAM were recorded at 286.08 eV (C–N) and 287.58 eV (C=O), corresponding with the record at 531.08 eV (C=O) in the O1s core-level, and for the N1s core-level peaks at 399.48 eV (C–N). For pNIPAM-NH_2 nanogels, the amine group (secondary) was confirmed by the record in N1s core-level peaks 401.48 eV ($-NH_2^+-$). From the XPS data, it has been confirmed that pNIPAM has been successfully functionalized with amine group. XPS analysis confirmed the presence of NH_2 on pNIPAM polymer by detecting the typical amine peak composing the backbone of the pNIPAM chain.

Antimicrobial activity of AgNP-polymeric nanoparticles

The antibacterial activities of the pNIPAM and pNIPAM-NH_2 AgNP-nanoparticles were evaluated against *E. coli* (Figures 9 and 10) and *S. aureus* (Figures 11 and 12). Briefly, for liquid culture, we added 40 µL of each AgNP-pNIPAM/pNIPAM-NH_2 nanoparticle to 160 µL of bacterial suspensions in LB broth during the exponential growth phase and monitored further bacterial growth by measuring the OD_{600} at 0, 1, 2, 3, 4, 5, and 24 h of culture. To evaluate antimicrobial activity on solid culture, 1×10 cells/mL suspension of bacterial cells was cultured on MH agar plate. An 8 mm punch was made on agar gel and 0.5 mg of (1 mg/mL) AgNP-pNIPAM/pNIPAM-NH_2 nanocomposite was loaded in the punch. The zone of inhibition for each set of composites was recorded after 24 h of incubation at 37°C. Our AgNP-pNIPAM/pNIPAM-NH_2 nanoparticles showed significant antimicrobial activities against both tested strains, but appeared more potent against *E. coli* (Figures 9 and 10) than previously reported.[41,42] The overall antimicrobial activities of all size groups (G1, G2, and G3) of the pNIPAM and pNIPAM-NH_2 AgNP-nanoparticles in liquid culture against *E. coli* were similar (Figures 9 and 10A–C), but in the solid culture, the difference between the zone of inhibition was more size-dependent (Figures 9 and 10D). The average diameter of the zones of inhibition caused by the pNIPAM AgNP G1, G2, and G3 groups against *E. coli* were 48±2, 36±2, and 28±2 mm and were higher than those against *S. aureus* (24±2.64, 20±4.58, 16±2.64 mm). In contrast, for pNIPAM-NH_2 AgNP with *E. coli*, the zone of inhibition for the G1, G2, and G3 groups were 58±8.71, 50±4.35, and 30±1 mm, respectively, while against *S. aureus* they were 27±2, 22±1, and 20±4.35 mm. The overall and pNIPAM-NH_2 AgNP antimicrobial effects were slightly higher, and differences in the antimicrobial activity at the last time point were observed because of their different AgNP concentrations and additional NH_2 group over the surface of the nanocomposite (Table 1). In addition, the antimicrobial effects of both types of AgNP-pNIPAM/pNIPAM-NH_2 nanoparticles against *S. aureus* (Figures 11 and 12) were lower than those for *E. coli*.

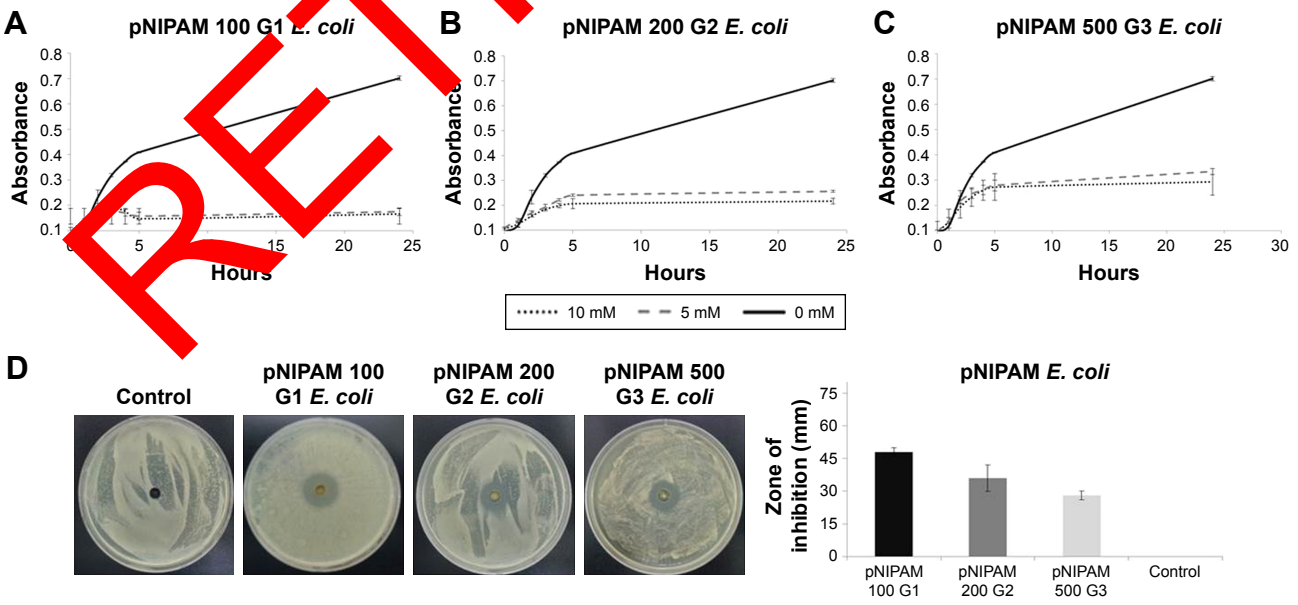

Figure 9 Antimicrobial activities of silver nanoparticle (AgNP)-encapsulated poly-*N*-isopropylacrylamide (pNIPAM) nanogel size groups G1–G3 against *Escherichia coli* (*E.coli*).
Notes: (**A**) Liquid culture of *E. coli* with pNIPAM G1. (**B**) Liquid culture of *E. coli* with pNIPAM G2. (**C**) Liquid culture of *E. coli* with pNIPAM G3. (**D**) Solid culture of *E. coli* with control (pure growth), pNIPAM G1–G3 and average diameter of zone of inhibition (mm) graph.

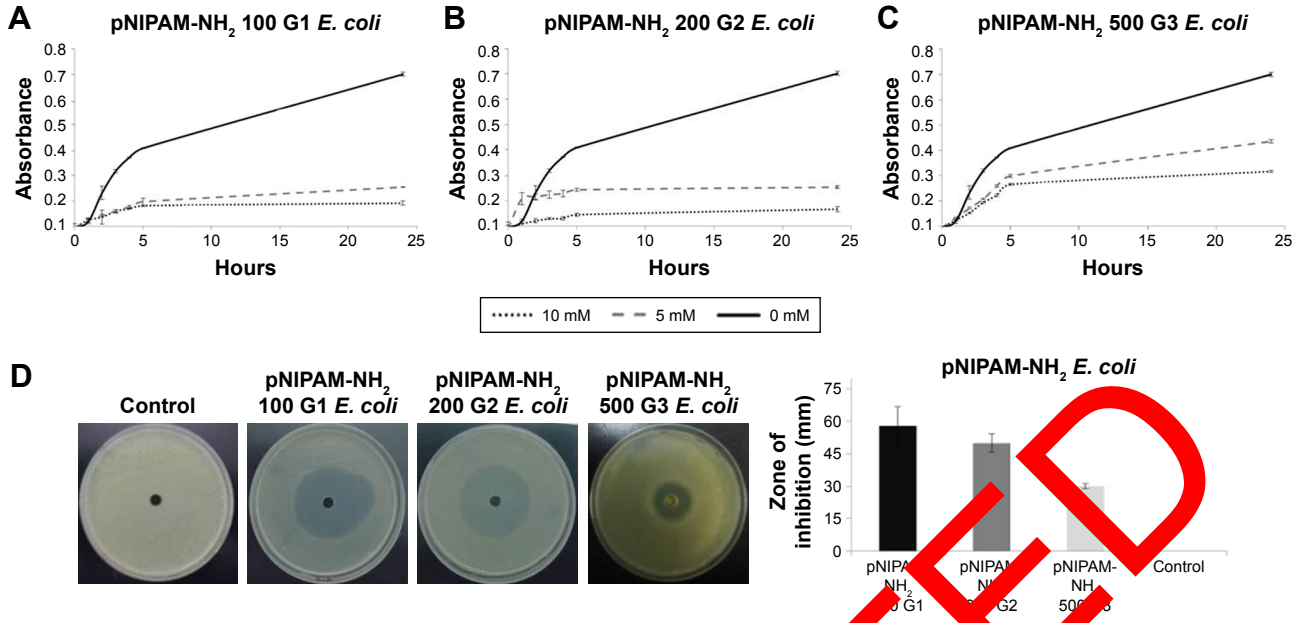

Figure 10 Antimicrobial activities of silver nanoparticle (AgNP)-encapsulated poly-*N*-isopropylacrylamide (p[illegible]-NH$_2$ nanogel [illegible] groups G1–G3 against *Escherichia coli* (*E. coli*).

Notes: (**A**) Liquid culture of *E. coli* with pNIPAM-NH$_2$ G1. (**B**) Liquid culture of *E. coli* with pNIPAM-NH$_2$ G2. (**C**) Liquid culture of *E. coli* with pNIPAM-NH$_2$ G3. (**D**) Solid culture of *E. coli* with control (pure growth), pNIPAM-NH$_2$ G1–G3 and average diameter of zone of inhibition (mm) graph.

In vitro cytotoxicity of AgNP-polymeric nanoparticles

One of the purposes of this study was to reduce the cytotoxicity of AgNPs in human cells. To evaluate the cytotoxicity of AgNP-polymeric nanoparticles, MTT assays with hASCs were performed. Figure 3 shows the in vitro cytotoxicities of pNIPAM and pNIPAM-NH$_2$ AgNP-nanoparticles in three size groups (G1, G2, and G3) against hASCs after 48 h. The results showed that smaller AgNP-polymeric nanoparticles had higher cytotoxicity (Figure 3). The cytotoxicities of the pNIPAM and pNIPAM-NH$_2$ AgNP-nanoparticles were higher in the AgNP-nanoparticles fabricated with the highest

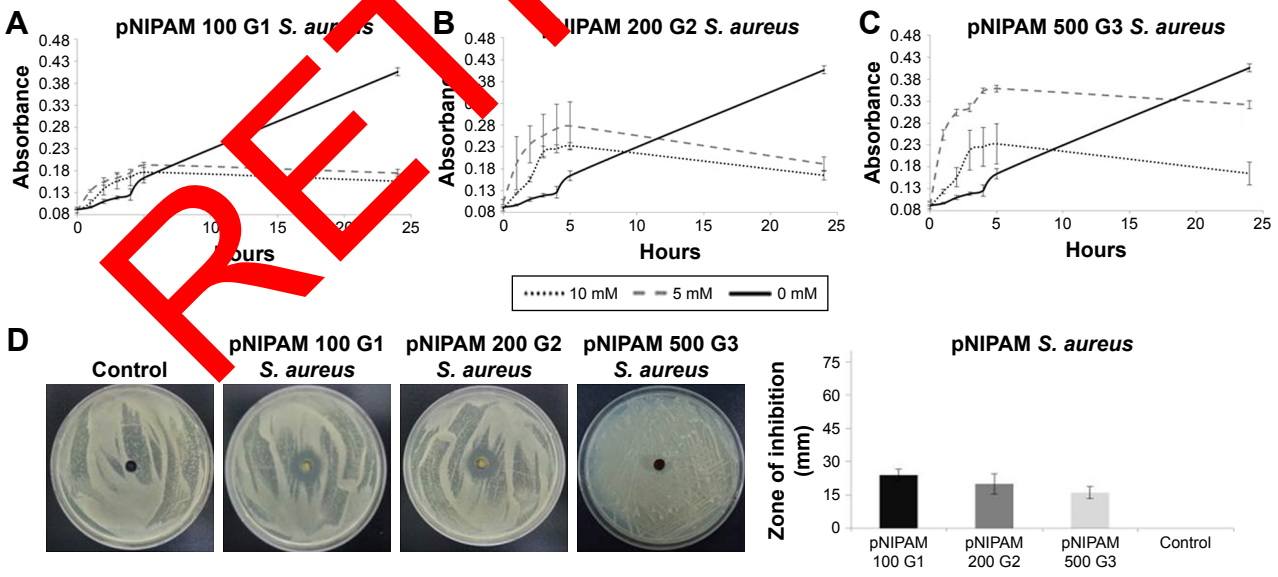

Figure 11 Antimicrobial activities of silver nanoparticle (AgNP)-encapsulated poly-*N*-isopropylacrylamide (pNIPAM) nanogel size groups G1–G3 against *Staphylococcus aureus* (*S. aureus*).

Notes: (**A**) Liquid culture of *S. aureus* with pNIPAM G1. (**B**) Liquid culture of *S. aureus* with pNIPAM G2. (**C**) Liquid culture of *S. aureus* with pNIPAM G3. (**D**) Solid culture of *S. aureus* with control (pure growth), pNIPAM G1–G3 and average diameter of zone of inhibition (mm) graph.

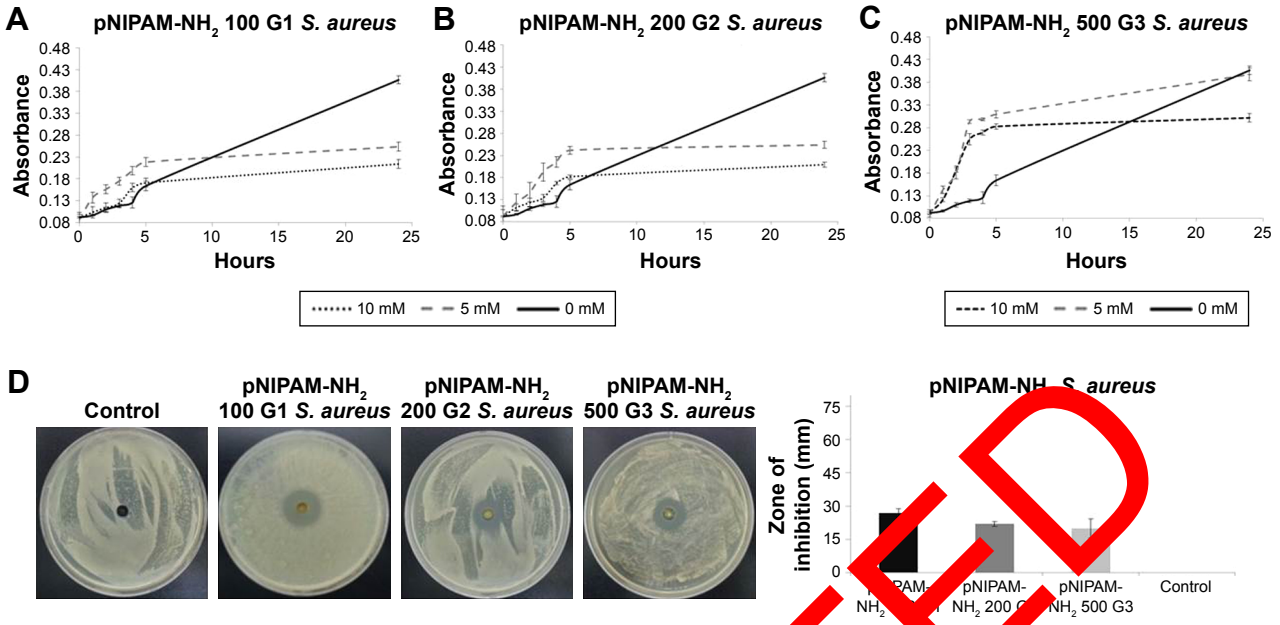

Figure 12 Antimicrobial activities of silver nanoparticle (AgNP)-encapsulated poly-*N*-isopropylacrylamide (pNIPAM)-NH_2 nanogel groups G1–G3 against *Staphylococcus aureus* (*S. aureus*).

Notes: (**A**) Liquid culture of *S. aureus* with pNIPAM-NH_2 G1. (**B**) Liquid culture of *S. aureus* with pNIPAM-NH_2 G2. (**C**) Liquid culture of *S. aureus* with pNIPAM-NH_2 G3. (**D**) Solid culture of *S. aureus* with control (pure growth), pNIPAM-NH_2 G1–G3 and average diameter of zone of inhibition (mm) graph.

concentration of $AgNO_3$ (10 mM). The largest (G3) AgNP-polymeric nanoparticles showed the lowest cytotoxicity, as smaller AgNP-polymeric nanoparticles have a greater ability to penetrate biological membranes because of their high surface area to charge ratio.[32] In addition, pNIPAM-NH_2 AgNP-nanoparticle groups showed higher cytotoxicities than pNIPAM AgNP-nanoparticles despite their lower Ag^+ concentration (Table 1). This may be because of the addition of the NH_2 surface charge as confirmed by XPS surface analysis (Figure 8).

Discussion

Characterization of AgNP-polymeric nanoparticles

AgNP-encapsulating pNIPAM/pNIPAM-NH_2 polymeric nanoparticles were synthesized by two step processes: synthesis of pNIPAM/pNIPAM-NH_2 nanoparticles via polymerization of NIPAM with the aid of BIS and APS, and 2) encapsulation of AgNPs inside of resulting polymeric nanoparticle networks using $AgNO_3$ solutions. DLS analysis revealed that an increase of NIPAM:BIS ratios increased the particle size of both pNIPAM and pNIPAM-NH_2 nanoparticles (Figure 1). The differences in size between the pNIPAM and pNIPAM-NH_2 nanoparticles were caused by the presence of the comonomer APMAAHC.[32] It is also speculated that addition of an NH_2 group to pNIPAM-NH_2 by using the APMAAHC comonomer resulted in extra hindrance and repulsion between consecutive NH_2 groups over the surface of nanogels, slightly increasing the nanogel size.[33] These results indicate that polymeric nanoparticle size can be modulated by changing the monomer to cross-linker ratio.

Table 1 Retention of silver after washing of pNIPAM and pNIPAM-NH_2 AgNP-nanoparticles as determined via ICP-OES analysis

Name of group	Concentration (Ag) µg/µL	Name of group	Concentration (Ag) µg/µL
pNIPAM-AgNPs G1 10 mM	0.01656	pNIPAM-NH_2-AgNPs G1 10 mM	0.01347
pNIPAM-AgNPs G1 5 mM	0.01271	pNIPAM-NH_2-AgNPs G1 5 mM	0.01068
pNIPAM-AgNPs G2 10 mM	0.0182	pNIPAM-NH_2-AgNPs G2 10 mM	0.01473
pNIPAM-AgNPs G2 5 mM	0.01335	pNIPAM-NH_2-AgNPs G2 5 mM	0.01219
pNIPAM-AgNPs G3 10 mM	0.02165	pNIPAM-NH_2-AgNPs G3 10 mM	0.0183
pNIPAM-AgNPs G3 5 mM	0.01541	pNIPAM-NH_2-AgNPs G3 5 mM	0.01327

Abbreviations: pNIPAM, poly-*N*-isopropylacrylamide; AgNP, silver nanoparticle; ICP-OES, inductively-coupled plasma optical emission spectrometry.

Similar to a previous study, the intensity of the spectral peaks in our study increased with the increase in $AgNO_3$ concentration, but the absorption peak positions remained at the same wavelengths.[43] In addition, broad peaks were observed for the AgNP-polymeric nanoparticles with larger AgNPs (Figures 4A and 5A). Our results are similar to those in a recent study that clearly revealed the formation of broad absorption peaks with an increase in the size of either pure AgNPs or AgNPs encapsulated in NIPAM-*N,N*-methylene-bis-acrylamide (NIPAM-MBA) gels.[26] In contrast, a plasmon absorption increment in the UV-visible spectrum indicates the formation of a greater number of nanoparticles.[25] In our study, the pNIPAM AgNP-nanoparticles (Figure 4B) exhibited slightly higher absorption values than the pNIPAM-NH_2 AgNP-nanoparticles (Figure 5B). These differences might be due to the differing retention of AgNPs inside the AgNP-nanoparticles after washing and the differences in Ag concentrations, as shown in the ICP-OES characterization in Table 1.

The histograms in Figure S1A and B indicate variations in AgNP size; however, the diameters of approximately 85% of the AgNPs were in the range of 1–10 nm. The TEM micrographs also show that the AgNPs were highly dispersed inside the AgNP-polymer nanoparticles and were mostly spherical in shape. Hence, optimization of the experimental conditions, including pH, the concentration of $AgNO_3$, nanoparticle size, and surface charge can achieve monodispersity and uniformity of shape.[44] Our aim was to obtain a uniform size distribution of AgNPs inside the AgNP-polymeric nanoparticles, and the method used produced ultra-small AgNPs with a well-controlled size distribution using $NaBH_4$ as the reducing agent. The chemical reaction for the $NaBH_4$ reduction of $AgNO_3$ is:

$$AgNO_3 + NaBH_4 \rightarrow Ag^0 + {}^{1/2}H_2 + {}^{1/2}B_2H_6 + NaNO_3$$

The major advantage of this in situ AgNP fabrication technique is that it provides size-controlled, uniformly sized, and homogeneously distributed nanoparticles inside a polymeric nanoparticle without the addition of a further stabilizer.[8] This is confirmed in Figures 5 and 6, which show that the nanoparticles were evenly distributed within the polymeric chain network. As expected, we observed homogeneous distributions of AgNPs throughout the AgNP-polymeric nanoparticles, even though there was a rapid reduction of Ag^+ into AgNPs by $NaBH_4$.[25]

Changing the size or alignment of AgNPs may be possible by modifying the polymeric nanoparticle network architecture.[13,45] This could be achieved by varying the ratio of monomer to cross-linker used when preparing the nanoparticle. Our results showed that the AgNPs formed in AgNP-polymeric nanoparticles with different monomer:cross-linker ratios were uniformly spherical and well dispersed, but they had different sizes depending on the size of the polymeric nanoparticle.

Antimicrobial activity

Most orthopedic infections are attributed to *Staphylococcus* spp., and *S. aureus* is the leading pathogen causing biomedical implant-related infections. *S. aureus* is often carried on the skin or in the nose of healthy people and readily adheres to host proteins (eg, fibrinogen, fibronectin) on biomaterials.[4] Such adherence can lead to the formation of a biofilm that protects the pathogen against antimicrobial agents. *S. aureus* is among the most frequently reported pathogens causing deep infections in hospitals. *E. coli* represents a diverse group of bacteria that reside in the intestines. Many *E. coli* strains are harmless, but some can cause diarrhea or illness outside the intestinal tract. In this study, we selected both *E. coli* and *S. aureus* to test the broad-spectrum antibacterial activities of our AgNP-pNIPAM/pNIPAM-NH_2 nanoparticles.

The results in Figures 9–12 exhibited the antimicrobial effects of our nanoparticle system against both *E. coli* and *S. aureus*. Interestingly, a higher antimicrobial effect against *E. coli* than *S. aureus* might be due to the structural difference in bacterial cell walls. The difference in the effect of Ag on Gram-negative and Gram-positive bacteria may lie in the structure of their cell walls. Gram-negative bacteria are encased in a thin, negatively charged outer lipopolysaccharide layer (7–8 nm thickness), whereas Gram-positive bacterial cell walls consist of a thick, highly cross-linked rigid peptidoglycan layer (20–80 nm thickness). The higher protection afforded by the Gram-positive cell wall may inhibit or prevent the bactericidal effect of AgNP-pNIPAM/pNIPAM-NH_2 nanoparticles. The greater susceptibility of Gram-negative bacteria to AgNP-pNIPAM/pNIPAM-NH_2 nanoparticles may also involve effects on bacterial signal transduction (ie, phosphorylation). Moreover, negative charges on lipopolysaccharides are attracted to the weak positive charge on AgNP-pNIPAM/pNIPAM-NH_2 nanoparticles.[46] Independently of bacterial type, the antibacterial properties of AgNP-pNIPAM/pNIPAM-NH_2 nanoparticles increased at higher concentrations of $AgNO_3$. However, polymeric nanoparticle size had a greater effect on antibacterial activity than $AgNO_3$ concentration, and thus the smallest AgNP-pNIPAM/pNIPAM-NH_2 nanoparticles

had the greatest antibacterial activities against both bacterial strains (Figures 9–12).

The antibacterial properties of our AgNP-polymeric nanoparticles were size-dependent. Smaller nanoparticles have a greater surface area to volume ratio and can more easily penetrate biological surfaces.[47,48] Our results showed that smaller G1 and G2 AgNP-polymeric nanoparticles had better antimicrobial activities than G3 AgNP-polymeric nanoparticles. The smaller AgNP-polymeric nanoparticles enable Ag-NPs to easily penetrate the cell wall, and their large surface area per mass brings a large number of atoms into contact with the ambient environment, resulting in an antibacterial material that is readily available to react with the components of bacterial cells.[40,32]

In particular, AgNP-polymeric nanoparticles with a high Ag content showed increased antimicrobial properties toward *E. coli* and *S. aureus*. The pNIPAM AgNP-nanoparticles showed a higher retention of Ag content after washing than the pNIPAM-NH_2 AgNP-nanoparticles (Table 1). The antimicrobial properties of AgNP-polymeric nanoparticles allow researchers to tune their use for specific applications. For instance, to prevent biofilm formation, a highly diffusive bactericidal agent loaded into a polymeric nanoparticle may be the most appropriate means of infection prevention. This tunable feature of AgNP-polymeric nanoparticles enables optimization of Ag release for specific clinical uses and infection types, allowing targeted drug delivery that can minimize complications with the use of antimicrobial agents.[49] Based on our results, AgNP-polymeric nanoparticles exhibit antimicrobial properties and may be useful in various biomedical applications.

In vitro cytotoxicity

The differences in cytotoxicity among AgNP-polymeric nanoparticles may arise from their different concentrations of Ag and different surface charges, eg, the high cytotoxicity of the Ag-NH_2 polymeric nanoparticle containing 10 mM $AgNO_3$ is governed by its high concentration of Ag^+ (Table 1). This is supported by the observation that pNIPAM and pNIPAM-NH_2 nanoparticles do not, on their own, exhibit cytotoxicity against hASCs.[10] The use of a lower concentration of $AgNO_3$ (5 mM) in both types of AgNP-polymeric nanoparticles resulted in a significantly higher survival of hASCs. Thus, our AgNP-polymeric nanoparticles developed using 5 mM $AgNO_3$ are suitable for contact with human tissues (Figure 3). The results suggest that cytotoxicity can be further reduced by optimizing the surface charge, in this case by adding NH_2 surface charge.

In conclusion, chemical synthesis methods for preparing AgNPs have been investigated in recent studies, with particular attention given to modifying their size and shape distributions. In the present study, the average sizes of the pNIPAM AgNP-nanoparticles were 131±78, 312±71, and 483±35 nm, while those of the pNIPAM-NH_2 AgNP-nanoparticles were 135±59, 174±10, and 532±48 nm for small, medium, and large size groups, respectively. Based on our results, AgNPs can be encapsulated within a polymer network. The AgNP-polymeric nanoparticles developed in this study showed antibacterial activities against *E. coli* and *S. aureus* that were dependent on the size and amount of AgNPs within the polymeric nanoparticle and polymeric nanoparticle's surface charge. These results suggest that our AgNP-polymeric nanoparticles may be used for antibacterial treatment to prevent postsurgical infections of biomedical implants.

Acknowledgments

This research was supported by the Korea Health Technology R&D Project through the Korea Health Industry Development Institute (KHIDI), funded by the Ministry of Health and Welfare, Republic of Korea (HI15C1744). This research was also supported by the Chung-Ang University Graduate Research Scholarship in 2016.

Disclosure

The authors report no conflicts of interest in this work.

References

1. Engemann JJ, Carmeli Y, Cosgrove SE, et al. Adverse clinical and economic outcomes attributable to methicillin resistance among patients with Staphylococcus aureus surgical site infection. *Clin Infect Dis*. 2003;36(5):592–598.
2. Zimmerli W, Ochsner PE. Management of infection associated with prosthetic joints. *Infection*. 2003;31(2):99–108.
3. Deyo RA, Nachemson A, Mirza SK. Spinal-fusion surgery – the case for restraint. *N Engl J Med*. 2004;350(7):722–726.
4. Lee JS, Murphy WL. Functionalizing calcium phosphate biomaterials with antibacterial silver particles. *Adv Mater*. 2013;25(8):1173–1179.
5. Pitout JD. The latest threat in the war on antimicrobial resistance. *Lancet Infect Dis*. 2010;10(9):578–579.
6. Berger RE. Emergence of a new antibiotic resistance mechanism in India, Pakistan, and the UK: a molecular, biological, and epidemiological study editorial comment. *J Urol*. 2011;185:154.
7. Makobongo MO, Gilbreath JJ, Merrell DS. Nontraditional therapies to treat Helicobacter pylori infection. *J Microbiol*. 2014;52(4):259–272.
8. Ramesh S, Sivasamy A, Rhee KY, et al. Preparation and characterization of maleimide–polystyrene/SiO2–Al2O3 hybrid nanocomposites by an in situ sol–gel process and its antimicrobial activity. *Composites Part B: Engineering*. 2015;75:167–175.
9. Shirkavand Hadavand B, Ataeefard M, Fakharizadeh Bafghi H. Preparation of modified nano ZnO/polyester/TGIC powder coating nanocomposite and evaluation of its antibacterial activity. *Composites Part B: Engineering*. 2015;82:190–195.

10. Prucek R, Tucek J, Kilianova M, et al. The targeted antibacterial and antifungal properties of magnetic nanocomposite of iron oxide and silver nanoparticles. *Biomaterials*. 2011;32(21):4704–4713.
11. Liu Z, Yan J, Miao YE, et al. Catalytic and antibacterial activities of green-synthesized silver nanoparticles on electrospun polystyrene nanofiber membranes using tea polyphenols. *Composites Part B: Engineering*. 2015;79:217–223.
12. Khan BA, Chevali VS, Na H, et al. Processing and properties of antibacterial silver nanoparticle-loaded hemp hurd/poly(lactic acid) biocomposites. *Composites Part B: Engineering*. 2016;100:10–18.
13. Wang C, Flynn NT, Langer R. Controlled structure and properties of thermoresponsive nanoparticle-hydrogel composites. *Adv Mater*. 2004; 16(13):1074–1079.
14. Kang YO, Im JN, Park WH. Morphological and permeable properties of antibacterial double-layered composite nonwovens consisting of microfibers and nanofibers. *Composites Part B: Engineering*. 2015;75: 256–263.
15. Liu F, Yuan Y, Li L, et al. Synthesis of polypyrrole nanocomposites decorated with silver nanoparticles with electrocatalysis and antibacterial property. *Composites Part B: Engineering*. 2015;69:232–236.
16. Silver S, Phung LT, Silver G. Silver as biocides in burn and wound dressings and bacterial resistance to silver compounds. *J Ind Microbiol Biotechnol*. 2006;33(7):627–634.
17. Johnson JR, Kuskowski MA, Wilt TJ. Systematic review: antimicrobial urinary catheters to prevent catheter-associated urinary tract infection in hospitalized patients. *Ann Intern Med*. 2006;144(2):116–126.
18. Abudabbus MM, Jevremović I, Janković A, et al. Biological activity of electrochemically synthesized silver doped polyvinyl alcohol/graphene composite hydrogel discs for biomedical applications. *Composites Part B: Engineering*. 2016;104:26–34.
19. Huang WF, Tsui GC, Tang CY, et al. Fabrication and process investigation of vancomycin loaded silica xerogel/polymer core–shell composite nanoparticles for drug delivery. *Composites Part B: Engineering*. 20 95:272–281.
20. Hao M, Tang M, Wang W, et al. Silver-nanoparticle-decorated multi walled carbon nanotubes prepared by poly(dopamine) funct alization and ultraviolet irradiation. *Composites Part B: Engin ng*. 2 6;95: 395–403.
21. Kim Y, Babu VR, Thangadurai DT, et al. Synthe Charac and Antibacterial Applications of Novel Cop meric Nanocomposite Hydrogels. *Bull Korean Chem Soc* 011;32:553 58.
22. Zare Y, Rhee KY, Hui D. Influence noparticles a gation/ agglomeration on the interfacial/in phase d tensile prop ties of nanocomposites. *Composites P B: Engineeri* 2017;122:41–46.
23. James C, Johnson AL, Jen s AT. Antimicrob surface grafted thermally responsive PN AM-co-A A nano-gels. *Chem Commun (Camb)*. 2011;47(48):1 7–1277
24. Surudžić R, Janković A, ik N, et al hysico–chemical and mechanical pro and a acterial tivity of silver/poly(vinyl alcohol)/gra ene na compo s btained by electrochemical method. *C posites P t B: Engine ing*. 2016;85:102–112.
25. Mohan Y Prem Geckeler KE. Fabrication of silver nanoparticles drogel networks. *Macromol Rapid Commun*. 2006; 27(16):1346–13
26. Kazimierska EA, szkowska M. Thermoresponsive poly-n-isopropylacrylamide gels modified with colloidal gold nanoparticles for electroanalytical applications. 1. Preparation and characterization. *Electroanalysis*. 2005;17(15–16):1384–1395.
27. Munkhbayar B, Bat-Erdene M, Sarangerel D, et al. Effect of the collision medium size on thermal performance of silver nanoparticles based aqueous nanofluids. *Composites Part B: Engineering*. 2013;54:383–390.
28. Nayak S, Bhattacharjee S, Chaudhary YS. In situ encapsulation and release kinetics of pH and temperature responsive nanogels. *J Phys Chem C*. 2012;116(1):30–36.
29. Hoare T, Pelton R. Functional group distributions in carboxylic acid containing poly(N-isopropylacrylamide) microgels. *Langmuir*. 2004; 20(6):2123–2133.
30. Nistor MT, Chiriac AP, Nita LE, et al. Upon the characterization of semi-synthetic hydrogels based on poly (NIPAM) inserted onto collagen sponge. *Composites Part B: Engineering*. 2012;43:1508–1515.
31. Omastová M, Mosnáčková K, Fedorko P, et al. Polypyrrole/silver composites prepared by single-step synthesis. *Synthetic Metals*. 2013; 166:57–62.
32. Qasim M, Baipaywad P, Udomluck N, Na D, Park H. Enhanced therapeutic efficacy of lipophilic amphotericin B against Candida albicans with amphiphilic poly(N-isopropylacrylamide) nanogels. *Macromol Res*. 2014;22(10):1125–1131.
33. Bagwe RP, Hilliard LR, Tan W. Surface modification of silica nanoparticles to reduce aggregation and nonspecif binding. *Langmuir*. 2006;22(9):4357–4362.
34. Wang W, Asher SA. Photochemical i orporation of ver quantum dots in monodisperse silica colloids f hotonic crysta pplications. *J Am Chem Soc*. 2001;123(50): 28–12 5.
35. Bhui DK, Bar H, Sarkar P, S oo GP, De S Misra A Synthesis and UV-vis spectroscopic st of silver anopart in aqueous SDS solution. *J Mol Liq*. 200 45(1): 57.
36. Choi JB, Park JS, d MS, Characte ation and antimicrobial property of poly ylic acid) na el cont ing silver particle prepared by electron b *t J Mol Sci*. 2 (6):11011–11023.
37. Xu ZP, Ze g QH, L Q, et al. Inorganic nanoparticles as carriers for efficient cellular delive *Chem Eng Sci*. 2006;61(3):1027–1040.
38. Da , Duening ML. C lytic nanoparticles formed by reduction c metal ions in multilayered polyelectrolyte films. *Nano Lett*. 2002; 5):497–501.
39. rphy CJ, Jana . Controlling the aspect ratio of inorganic nanorods an anowires. *Mater*. 2002;14(1):80–82.
40. van D P d CH, Binh LT, Kasbohm J. Chemical synthesis and ntibacterial activity of novel-shaped silver nanoparticles. *Int Nano* 12;2:9.
41. Alarcon EI, Udekwu K, Skog M, et al. The biocompatibility and antibacterial properties of collagen-stabilized, photochemically prepared silver nanoparticles. *Biomaterials*. 2012;33(19):4947–4956.
42. Taglietti A, Diaz Fernandez YA, Amato E, et al. Antibacterial activity of glutathione-coated silver nanoparticles against Gram positive and Gram negative bacteria. *Langmuir*. 2012;28(21):8140–8148.
43. Thomas V, Yallapu MM, Sreedhar B, Baipai SK. A versatile strategy to fabricate hydrogel-silver nanocomposites and investigation of their antimicrobial activity. *J Colloid Interface Sci*. 2007;315(1):389–395.
44. Fayaz AM, Balaji K, Girilal M, Yadav R, Kalaichelvan PT, Venketesan R. Biogenic synthesis of silver nanoparticles and their synergistic effect with antibiotics: a study against Gram-positive and Gram-negative bacteria. *Nanomedicine*. 2010;6(1):103–109.
45. Zhang JG, Xu SQ, Kumacheva E. Polymer microgels: reactors for semiconductor, metal, and magnetic nanoparticles. *J Am Chem Soc*. 2004;126(25):7908–7914.
46. Sui ZM, Chen X, Wang LY, et al. Capping effect of CTAB on positively charged Ag nanoparticles. *Physica E-Low-dimensional Systems and Nanostructures*. 2006;33(2):308–314.
47. Panacek A, Kvitek L, Prucek R, et al. Silver colloid nanoparticles: synthesis, characterization, and their antibacterial activity. *J Phys Chem B*. 2006;110(33):16248–16253.
48. Morones JR, Elechiguerra JL, Camacho A, Holt K, Kouri JB, Ramírez JT, Yacaman MJ. The bactericidal effect of silver nanoparticles. *Nanotechnology*. 2005;16(10):2346–2353.
49. Coll Ferrer MC, Dastghey S, Hickok NJ, Eckmann DM, Composto RJ. Designing nanogel carriers for antibacterial applications. *Acta Biomater*. 2014;10(5):2105–2111.

Supplementary material

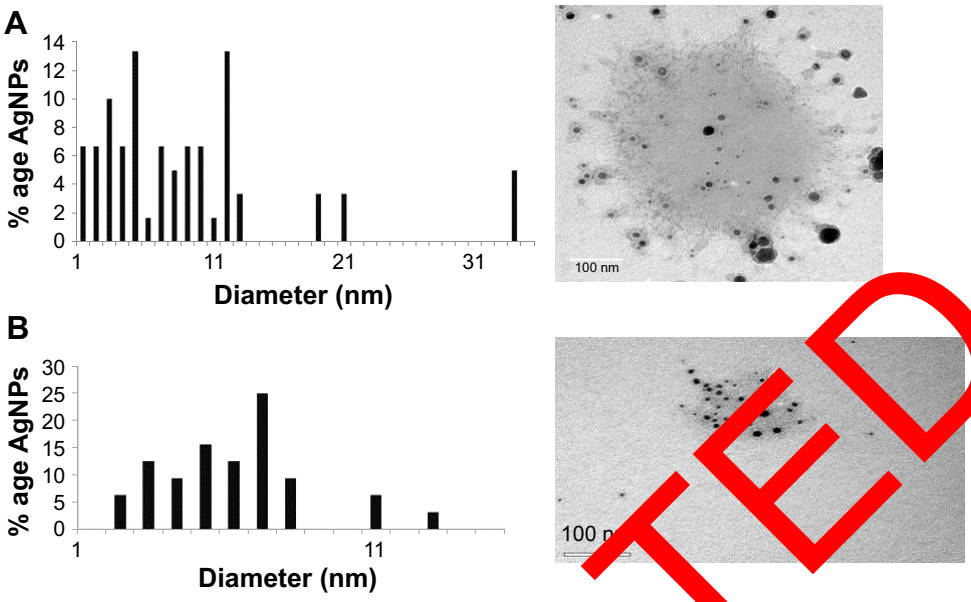

Figure S1 (**A**, **B**) Average diameter of AgNP inside the nanogels.
Abbreviation: AgNPs, silver nanoparticles.